ARISTOTLE UNIVERSITY OF THESSALONIKI

Development of a muon tomography application with MICROMEGAS detectors.

Amperiadou Dimitra

On behalf of the AUTh Muon Tomography team,
Ch. Petridou, D. Sampsonidis, S. Tzamarias, K.Kordas, Ch. Lampoudis, A. Leisos, A. Tsirigotis, Ch. Tsiafis.

HEP Conference, Thessaloniki, Greece
15th -19th June.

Presentation Outline

- **Introduction**
- The experimental set-up in the laboratory
- Data Analysis
  - Track Reconstruction
  - Back Projection Method
  - Results
- Conclusions and future work

Introduction

- Muon Tomography is a technique that uses cosmic ray muons for the imaging of large volumes.
- ***Muon Transmission Radiography (MT)*** ⟶ It exploits the dependence of the attenuation of the radiation of the thickness and density of the matter traversed.
- ***Muon Scattering Tomography (MS)*** ⟶ It is based on multiple Coulomb scattering of muons when they pass through a material of high-Z.
- Applications: Geology, Archaeology, Nuclear safety and security.

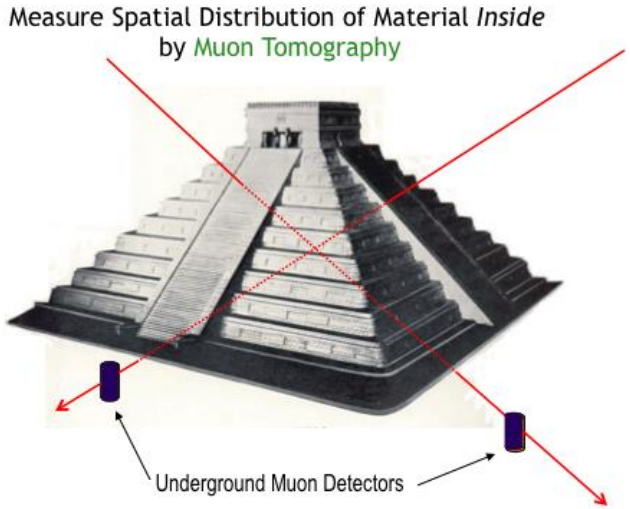

Figure 1: Search for hidden chambers in Chephren's pyramid by L.W. Alvarez and his team.

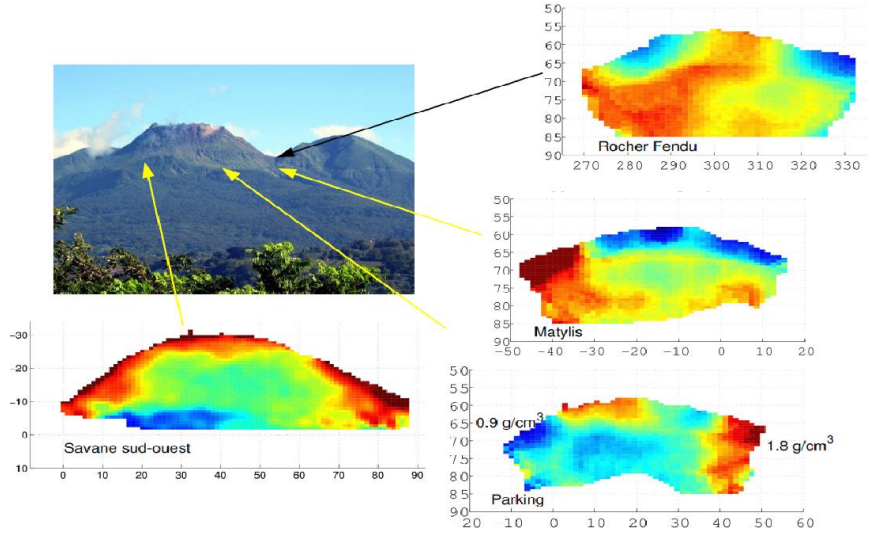

Figure 2: Structural imaging of the La Soufriere of Guadeloupe dome.

Luis W. Alvarez, Jared A. Anderson, F. El Bedwei, James Burkhard, Ahmed Fakhry, Adib Girgis, AmrGoneid, Fikhry Hassan, Dennis Iverson, Gerald Lynch, and et al. Search for hidden chambers in the pyramids.

Bonechi, L., D'Alessandro, R., & Giammanco, A. (2020). Atmospheric muons as an imaging tool. Reviews in Physics, 5.

Presentation Outline

- Introduction
- **The experimental set-up in the laboratory**
- Data Analysis
  - Track Reconstruction
  - Back Projection Method
  - Results
- Conclusions and future work

The experimental set-up in the laboratory

The goal of this experiment is to apply the muon tomography technique in a small scale, for the imaging of a lead cube of 5 cm.

The experimental setup consists of: 4 MICROMEGAS detectors and 3 scintillators.

- Top scintillator 10 cm x 11 cm.
- Four MICROMEGAS detectors with 2D redout (x-y),
  active area 10 cm x 10 cm and pitch=250 μm.

The distance between two MICROMEGAS is 7 cm.

- Middle scintillator 41 cm x 41 cm.
- 20 cm thick block of lead.
- Bottom scintillator 41 cm x 41 cm.

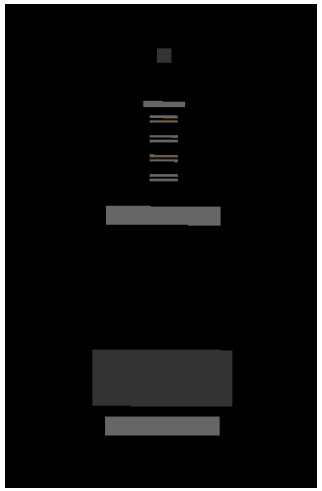

Figure 3: The geometry of the set-up in GEANT4.

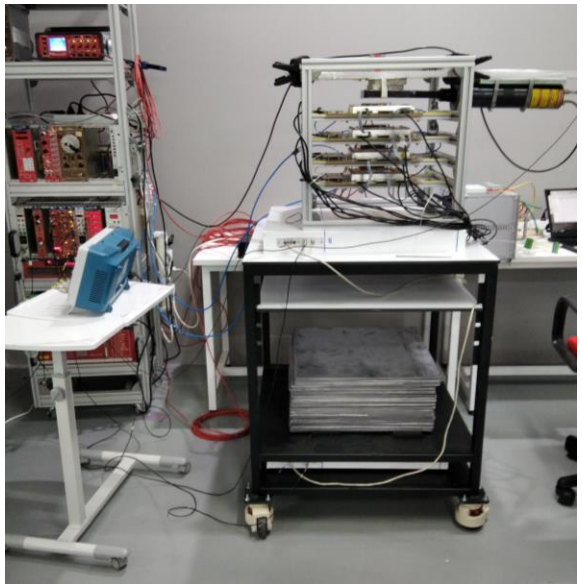

Figure 4: The experimental set-up in the laboratory.

- Signal on 1st and 2nd scintillator simultaneously: Double Coincidence (Trigger events)
- Signal on 1st, 2nd and 3rd scintillator: Triple Coincidence
- VETO: Signal from bottom scintillator vetos the double coincidence.

--> Focus on low energy muons, which are more likely to be absorbed in the lead cube.

The cube was initially placed at a distance of 130 mm from the upper MICROMEGAS and then at a distance of 230 mm.

Data were collected with and without the cube for the two cases.

Presentation Outline

- Introduction
- The experimental set-up in the laboratory
- Data Analysis
  - Track Reconstruction
  - Back Projection Method
  - Results
- Conclusions and future work

Data Analysis-Track reconstruction

- The reconstruction of muons' tracks is performed by using the hit position in every tracking detector (on xz and yz plane).
- Events with signal in all four detectors and with less than five clusters in every detector are considered.
- For events with more than one cluster in a layer, the tracking becomes challenging->Tracking Algorithm.

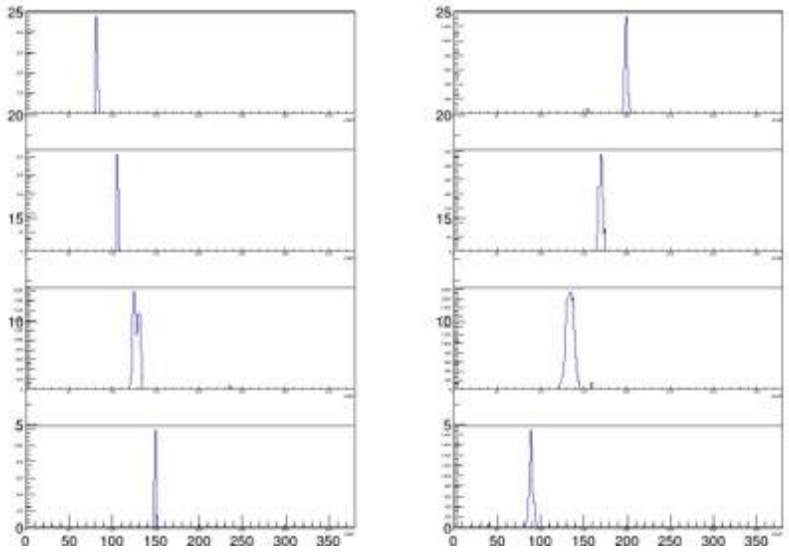

Figure 5: Event with one cluster in every detector.

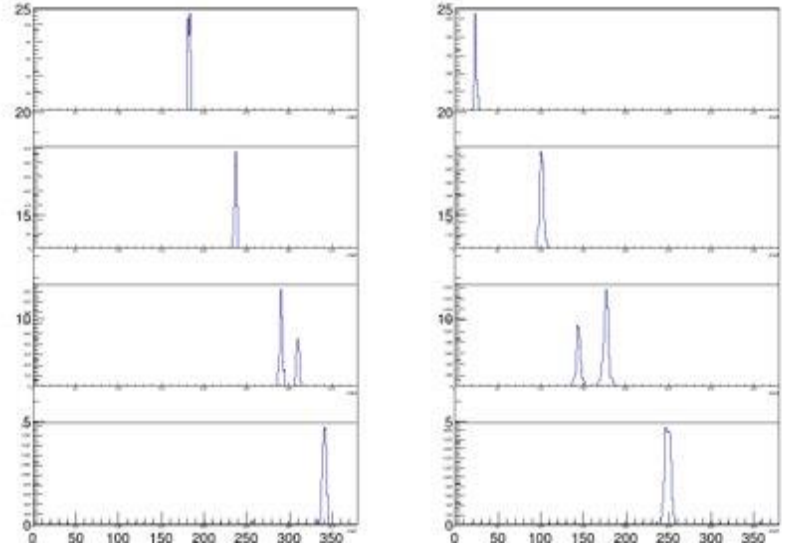

Figure 6: Event with more than one clusters in a detector.

Data Analysis-Track reconstruction.

The tracking algorithm.

- An iterative algorithm developed inspired by The Chain Algorithm, which gives one track per event (best χ^2) .

Bortfeldt, Jonathan. (2015). The Floating Strip Micromegas Detector.

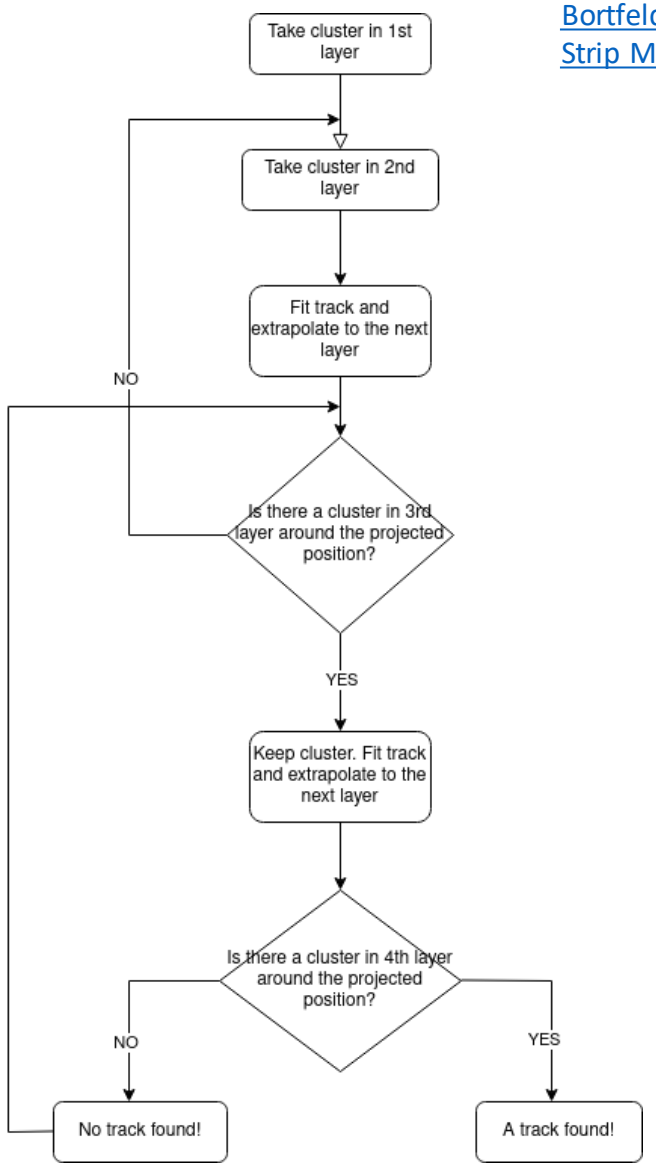

Figure 7: Flowchart of the tracking algorithm.

Data Analysis- Track reconstruction

The distribution of χ^2 .

Run with cube:
Total events: 38305 events.
Total reconstructed tracks: 28322 tracks.

Run without cube:
Total events : 47700 events.
Total reconstructed tracks: 34689 tracks.

In 1st run:

The cube was placed 130 mm above the top detector.

Total days of data acquisition: 12 days.

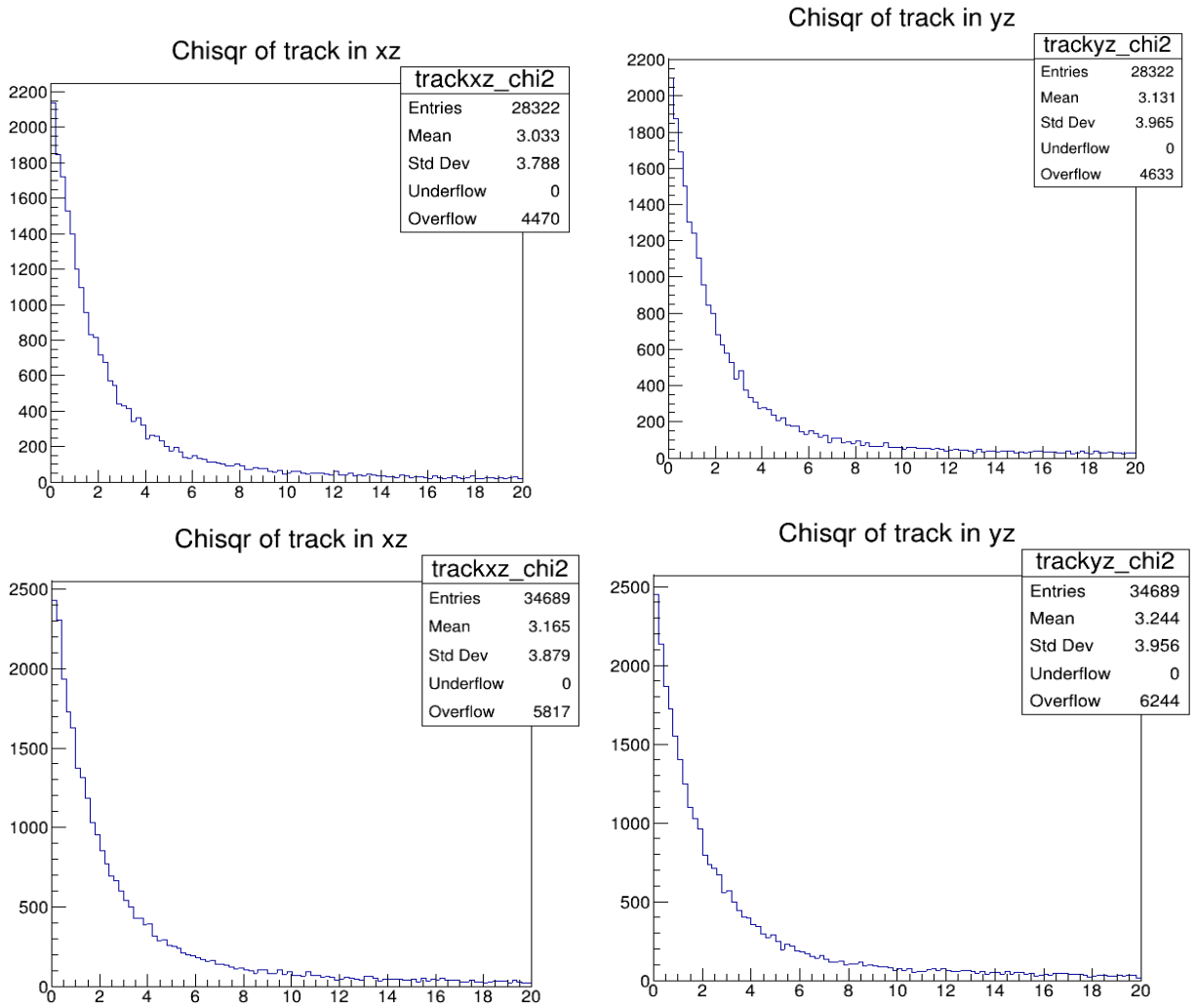

Figure 8: The distribution of χ2 of reconstructed tracks with cube (top) and without cube (bottom).

Amperiadou Dimitra, AUTh

Data Analysis- Track reconstruction

The distribution of χ2.

Run with cube:
Total events: 90369 events.
Total reconstructed tracks: 60424 tracks.

Run without cube:
Total events: 102610 events.
Total reconstructed tracks: 69183 tracks.

In 2nd run:

The cube was placed 230 mm above the top detector.

Total days of data acquisition: 27 days

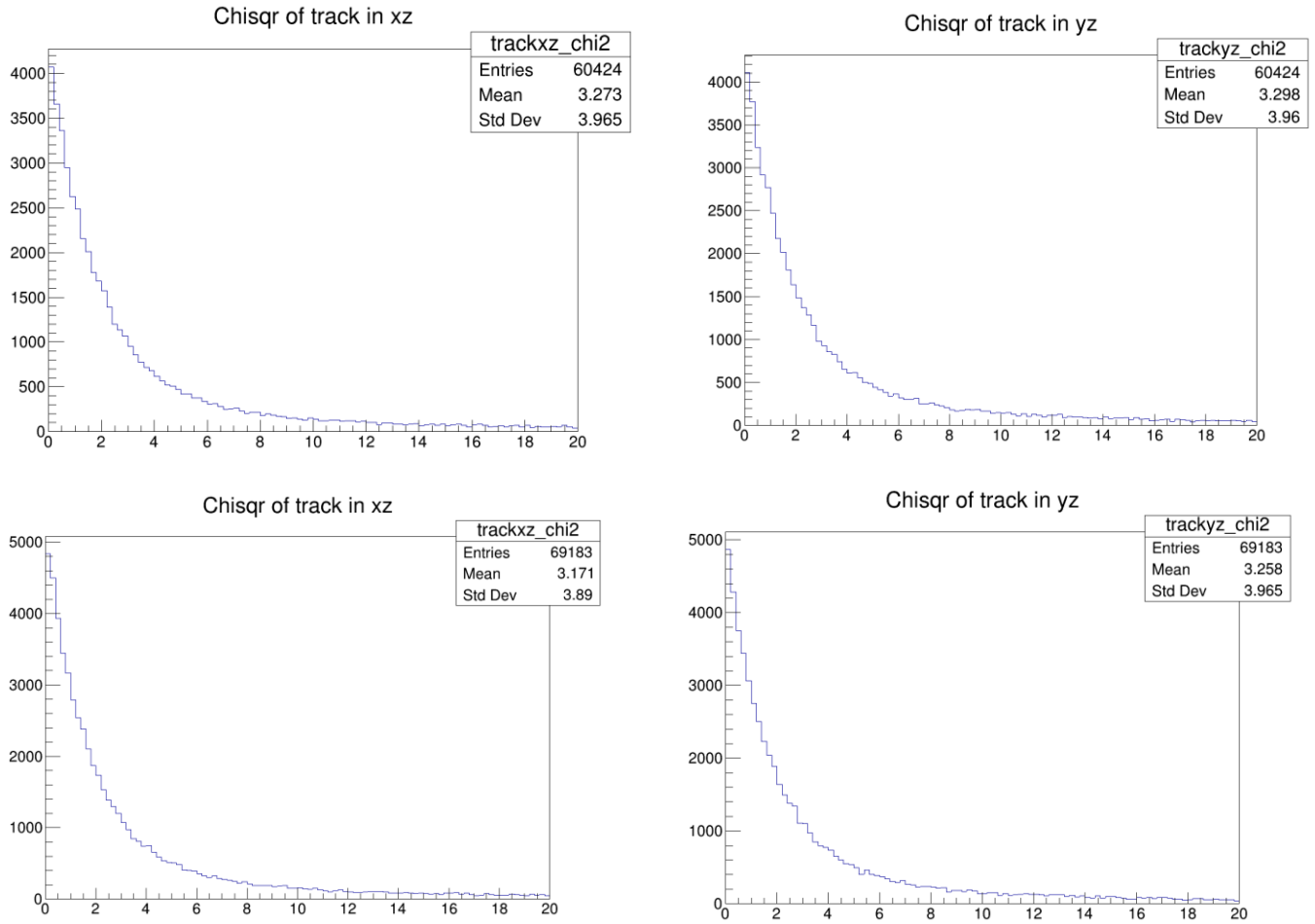

Figure 9: The distribution of χ2 of reconstructed tracks with cube (top) and without cube (bottom).

Data Analysis-Track reconstruction

Angular distribution from reconstructed tracks.

The analyzed data come from **Triple Coincidence events.**

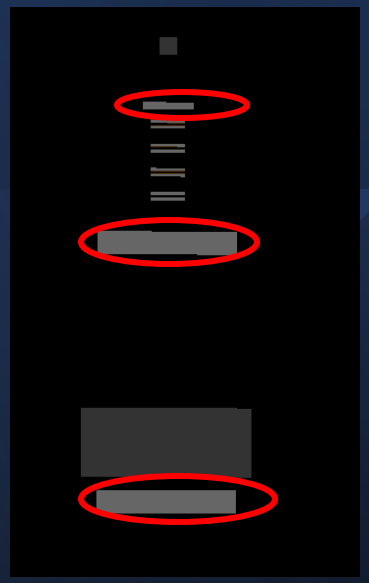

Figure 12: The geometry of the experimental set-up with scintillators marked.

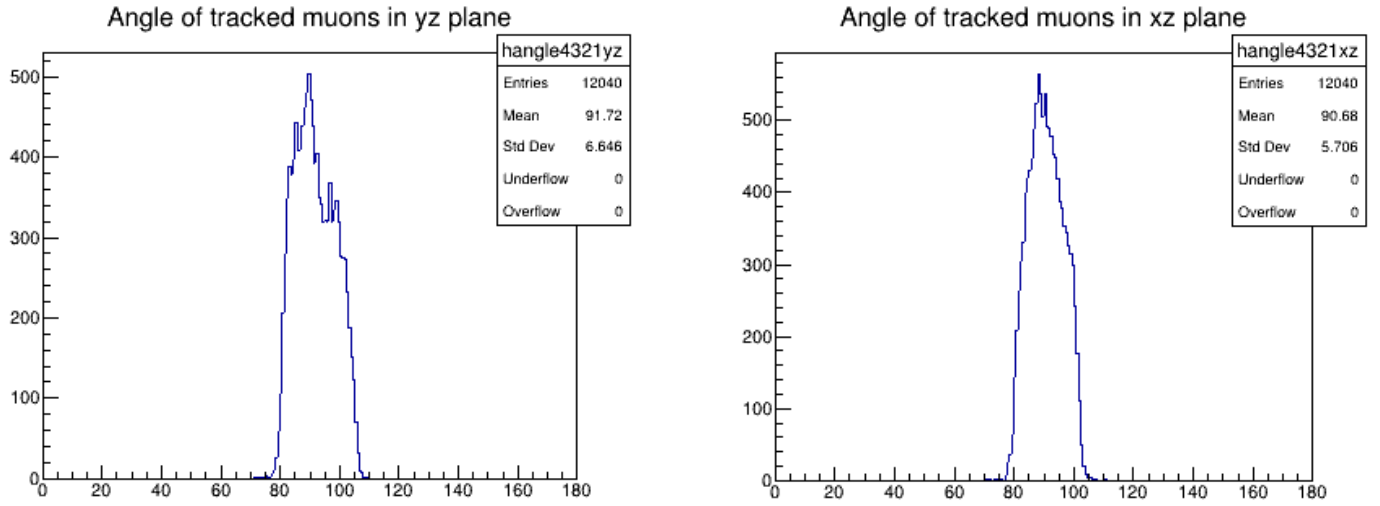

Data

Figure 13: Angular distribution (deg) from reconstructed tracks in triple coincidence events (data).

The acceptance of the three scintillators is about 75°-105°.

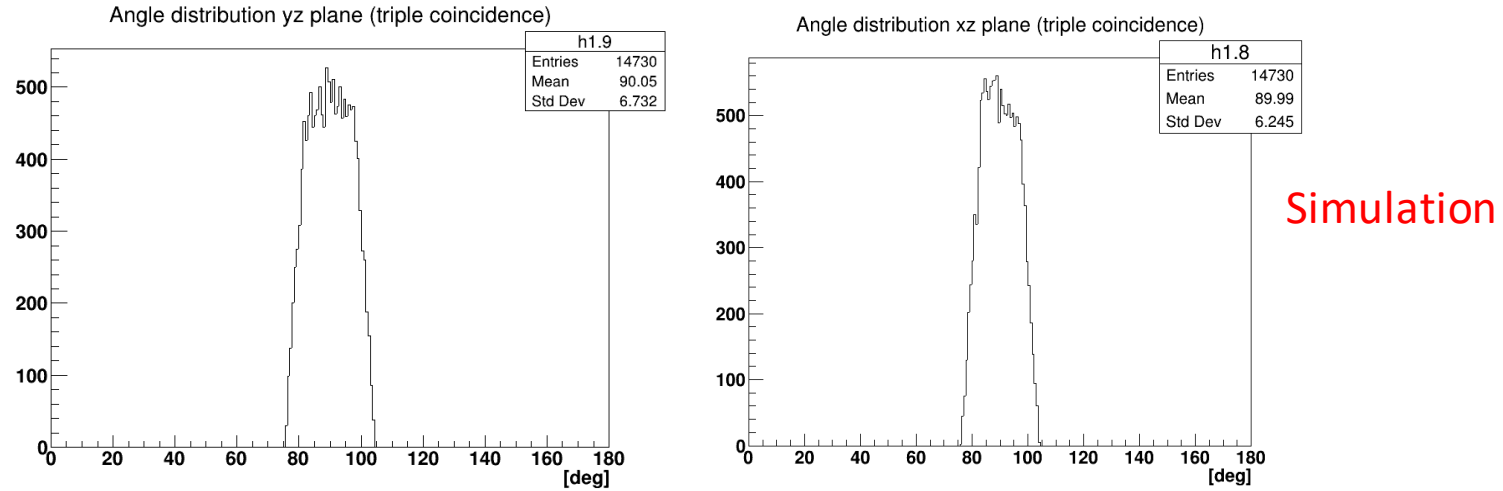

Simulation

Figure 14: Angular distribution from reconstructed tracks in triple coincidence events (simulation).

Amperiadou Dimitra, AUTh

Data Analysis-Track reconstruction

Angular distribution from reconstructed tracks.

The analyzed data come from **Double Coincidence events with VETO operation=ON**.

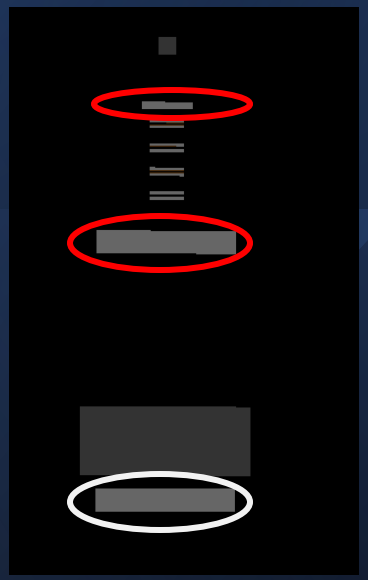

Figure 10: The geometry of the experimental set-up with scintillators marked.

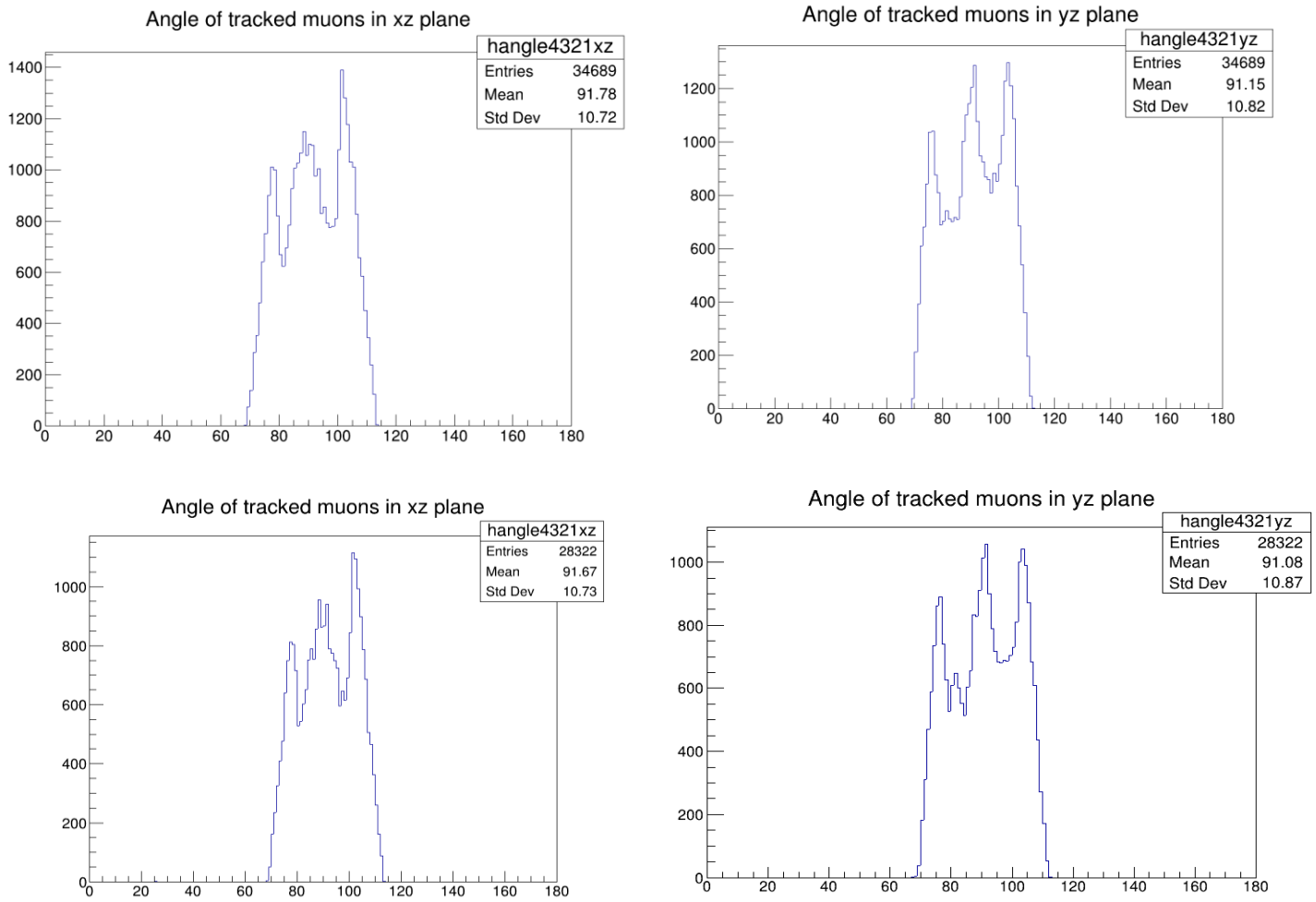

Figure 11: Angular distribution (deg) from reconstructed tracks without cube (top) and with cube (bottom) (**data-1st run**).

Presentation Outline

- Introduction
- The experimental set-up in the laboratory
- Data Analysis
  - Track Reconstruction
  - Back Projection Method
  - Results
- Conclusions and future work

Back Projection Method

- Ideal method for the imaging of underground objects or, objects surrounded by a material of different density.
- The detector's dimensions should not be negligible with respect to the object one.
- Trace back the muon trajectories on projection planes parallel to the detector.
- An optimal distance is found, where the image under study appears "focused" and the smearing is minimum. This distance is approximately the physical distance between the detector and the object.
- The angle λ(x), defined by the intersection of the vertical lines (parallel to z axis) with the limitations of the signal region in "zone 1" and "zone 2" respectively, shows a minimum at this distance where the transition from "zone 1" to "zone 2" takes place (location of the object).
- If the following inequality is satisfied, the angle λ reaches a minimum value.

$$\frac{d_r}{2}\frac{L-l_r}{d-L/2}-l_r<0$$

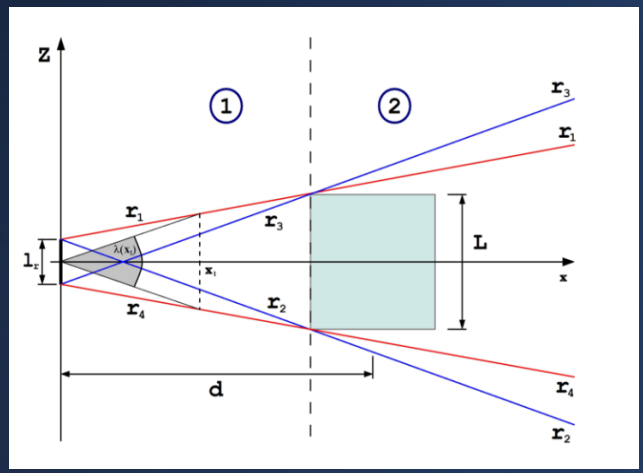

Figure 15: A schematic view of a cube-shaped object (side L), placed along the hodoscope axis at a distance d.

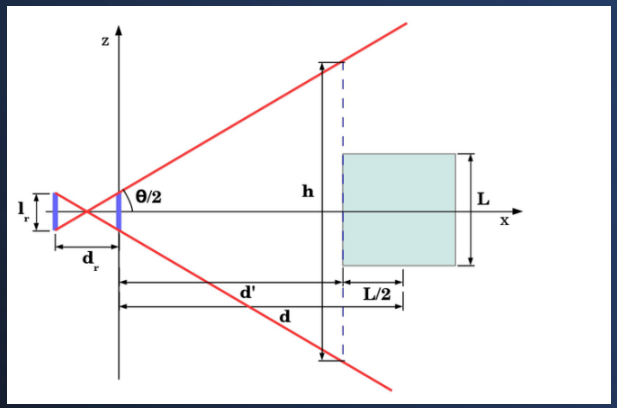

Figure 16: Schematic drawing showing the aperture (h) of the hodoscope relative to the side of the structure (L) .

Back Projection Method

- The bin size (pitch) of the back-projection planes scales linearly with the distance between the center of the plane and the center of the top detector: $p(x)=p_0+\delta_\theta x$.
- Back projection planes: 2D histograms (x/p,y/p) with and without the object.
- Get the subtraction (h_{nocube}-h_{cube}) and divide by the sum (h_{nocube}+h_{cube}) for each bin->2D histograms.
- Instead of using the angle λ(x), we can use the width-to-pitch ratio R(x).
- "Zone 1":

$$R_1(x)=\frac{w_1(x)}{p(x)}=\frac{1}{\delta_\theta x+p_0}\left[\frac{L-l_r}{d-L/2}x+l_r\right], \qquad x<d-L/2$$

$$\frac{\partial R_1(x)}{\partial x}=\frac{1}{(\delta_\theta x+p_0)^2}\left[\frac{L-l_r}{d-L/2}p_0-l_r\delta_\theta\right], \qquad x<d-L/2$$

- "Zone 2":

$$R_2(x)=\frac{w_2(x)}{p(x)}=\frac{1}{\delta_\theta x+p_0}\left[\frac{L+l_r}{d-L/2}x-l_r\right], \qquad x>d-L/2.$$

$$\frac{\partial R_2(x)}{\partial x}=\frac{1}{(\delta_\theta x+p_0)^2}\left[\frac{L+l_r}{d-L/2}p_0+l_r\delta_\theta\right], \qquad x>d-L/2.$$

The width-to-pitch ratio R(x) reaches a minimum value when $\frac{\partial R_1(x)}{\partial x}<0$ ⇒ $\frac{d_r}{2}\frac{L-l_r}{d-L/2}-l_r<0.$

($\delta\theta=2p_0/d_r$)

The minimum of width-to-pitch ratio: Location of the object.

The FWHM at the minimum: Dimensions of the object.

Bonechi, L., D'Alessandro, R., Mori, N., & Viliani, L. (2015). A projective reconstruction method of underground or hidden structures using atmospheric muon absorption data. Journal of Instrumentation.

Back projection Method

Spatial resolution of the detector.

- For the determination of the pitch size of every back projection plane, we need the spatial resolution of a single tracking plane (p_0) → $p(x)=p_0+\delta\theta*x$.

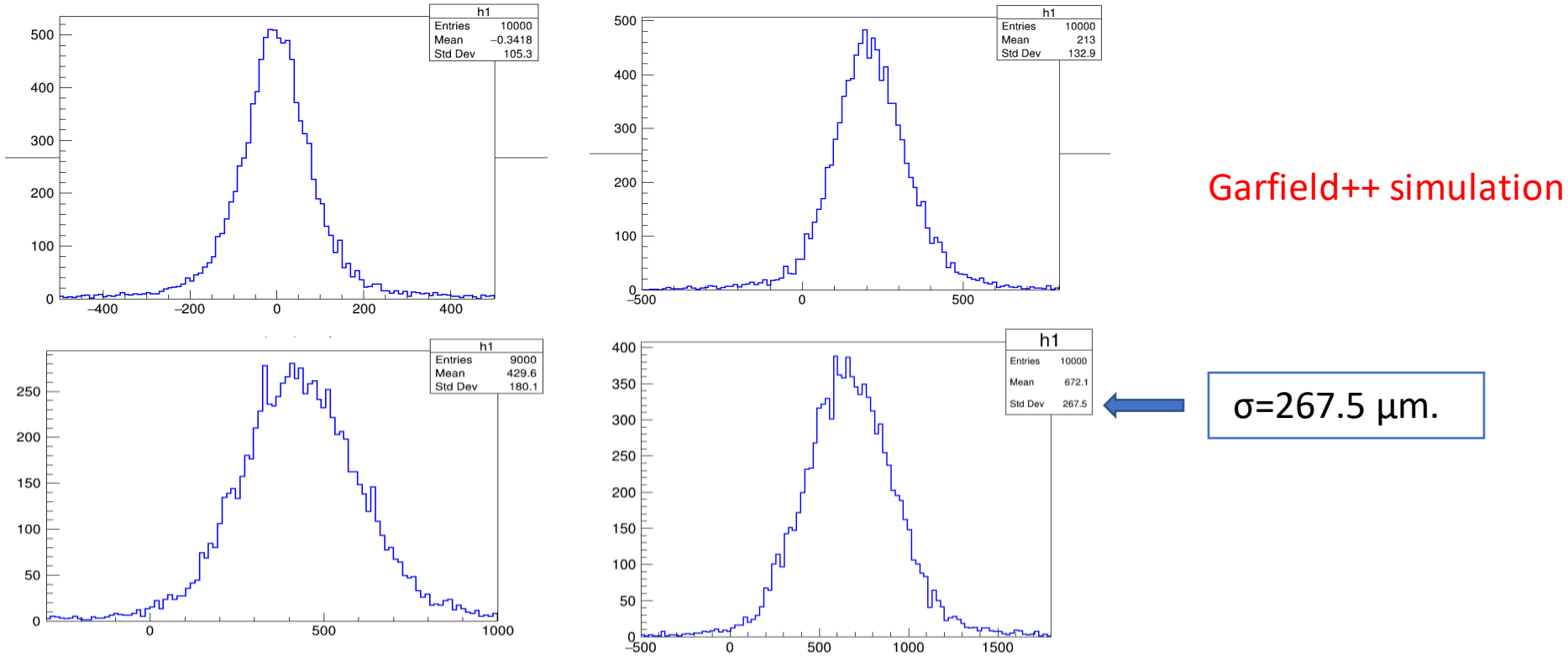

Figure 17: The distribution of the residuals (in μm) for (a) vertical tracks, (b) tracks with slope 95 deg, (c) tracks with slope 100 deg and (d) tracks with slope 105deg. (simulated data).

Presentation Outline

- Introduction
- The experimental set-up in the laboratory
- Data Analysis
  - Track Reconstruction
  - Back Projection Method
  - Results
- Conclusions and future work

Results

*1st run-cube placed **130 mm** from top detector.*

Determination of the object's distance from the top detector.

From fitted function:
D^{x}_{min}=84.32 ± 4.47 mm.
D^{y}_{min}=131 ± 7.03 mm.

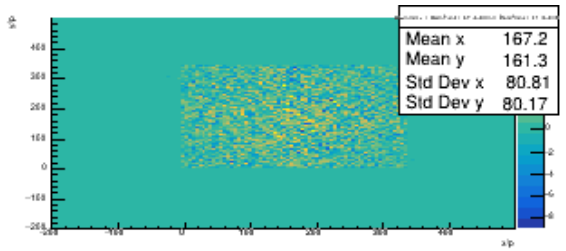

(a) distance=0 mm

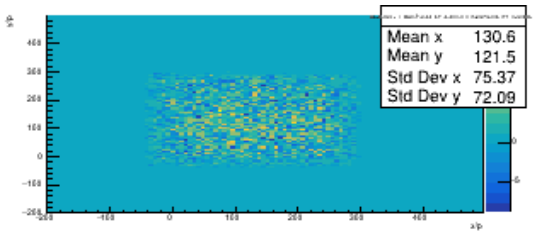

(b) distance=60 mm

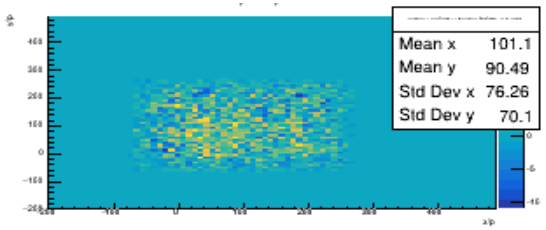

(c) distance=140mm

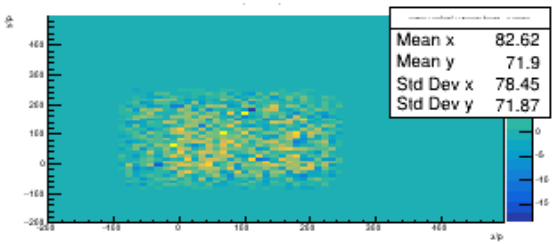

(d) distance=200mm

Figure 18: The three figures, corresponding to the projections back to three different planes, after subtraction.

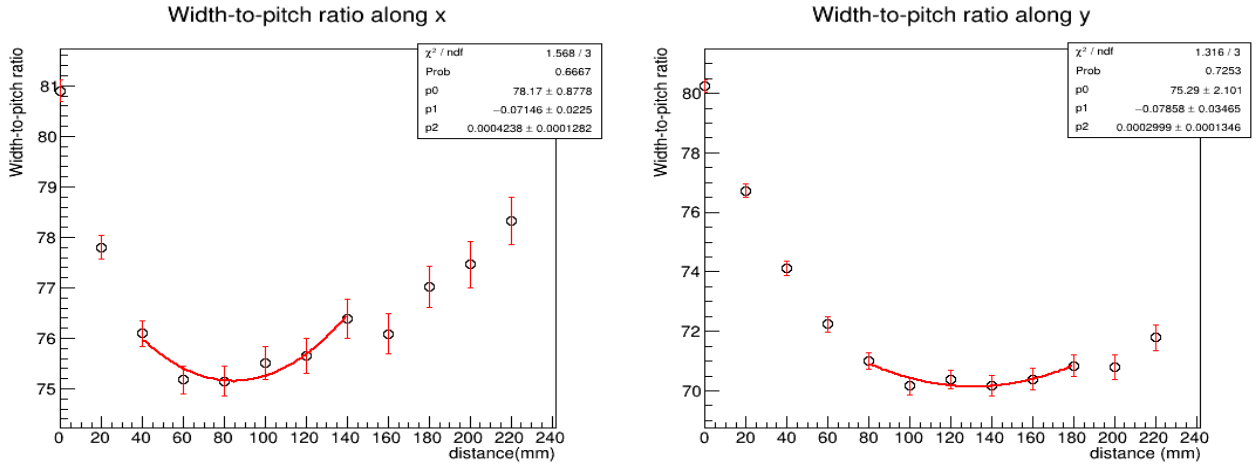

Figure 19: Width over pitch ratios for the distribution along the x axis (left) and the y axis (right) as a function of the distance from the detector to the projection plane, after subtraction. The distribution is fitted with a 2nd order polynomial in the interval around minimum.

Results

1st run

Determination of the cube's width.

real width=50 mm.

At D^x= 84.32 mm and D^y=131 mm:

$FWHM^x$= 67.08 ± 2.16 mm.
$FWHM^y$ = 72.58 ± 1.65 mm.

$2\sigma^x$= 56.97 ± 1.99 mm.
$2\sigma^y$=61.64 ± 1.46 mm.

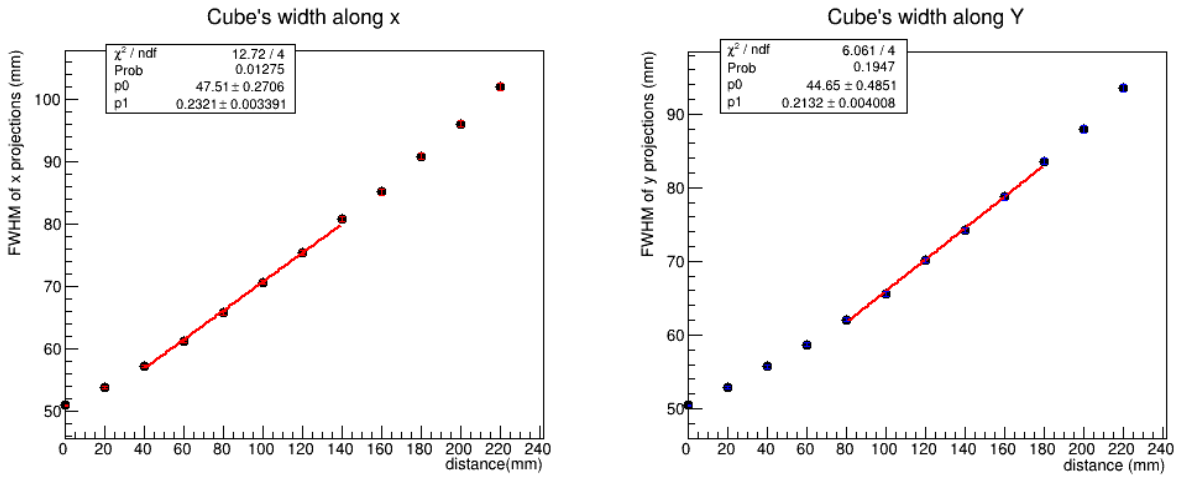

(a) The FWHM (mm) of x (left) and y (right) projections.

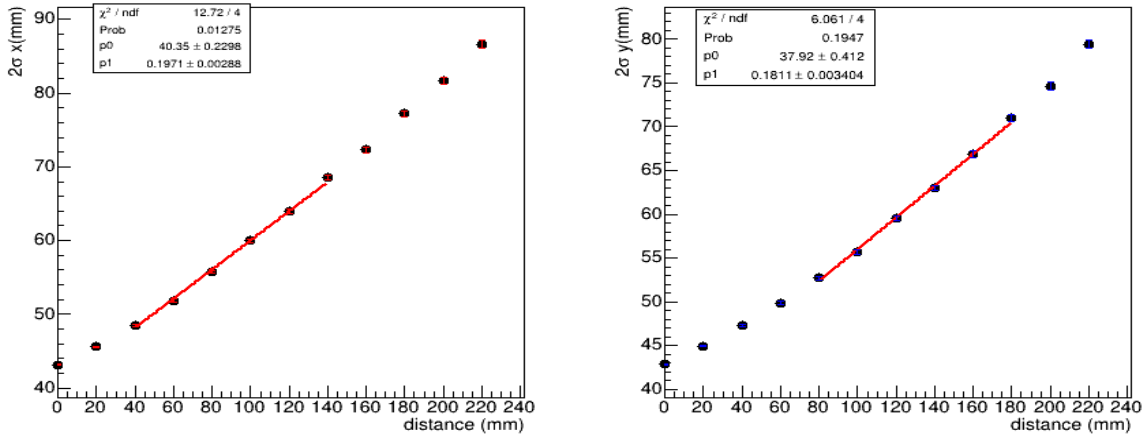

(b) 2σ (mm) of x (left) and y (right) projections.

Figure 20: (a)The FWHM(mm) and (b) The 2σ (mm) of the projections along x (left) and along y (right) as a function of distance (mm) in 1st run.

Results

*2nd run-cube placed **230 mm** from top detector.*

Determination of the object's distance from the top detector.

From fitted function:
D^{x}_{min}=266.06 ± 9.36 mm.
D^{y}_{min}=242.86 ± 8.046 mm.

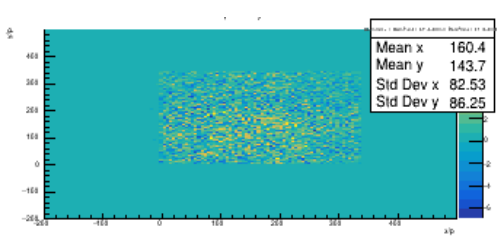

(a) distance=30 mm

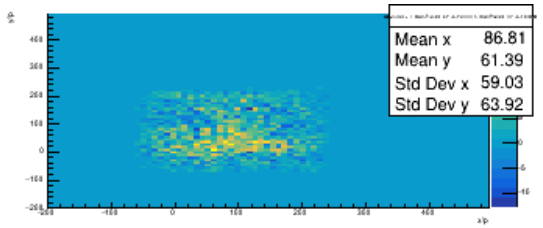

(b) distance=150mm

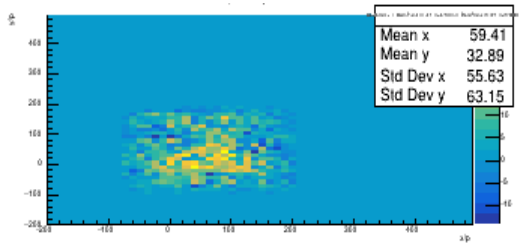

(c) distance=270 mm

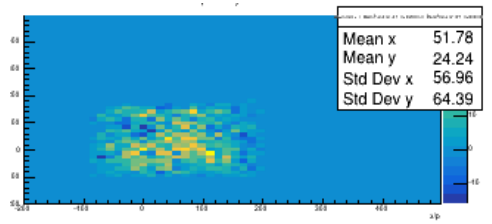

(d) distance=330 mm

Figure 21: The three figures, corresponding to the projections back to three different planes, after subtraction.

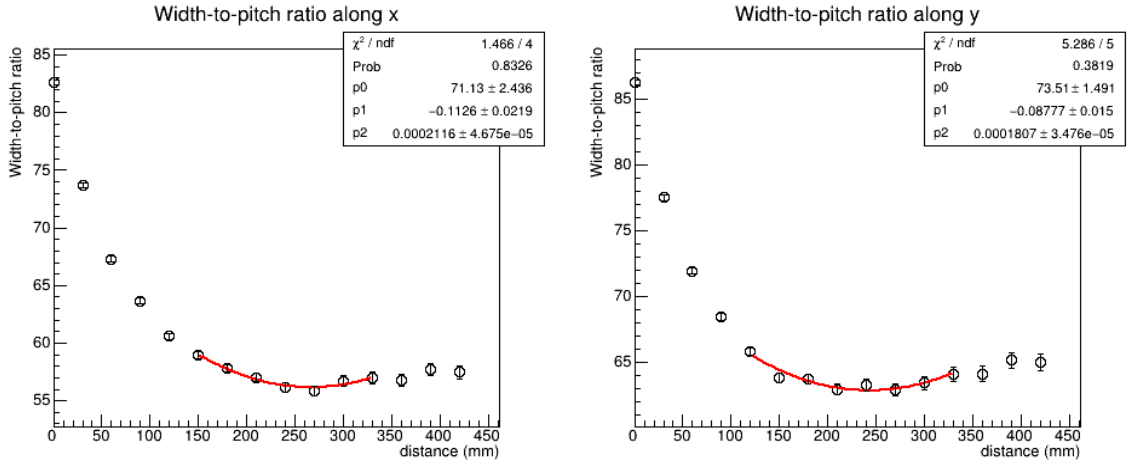

Figure 22: Width over pitch ratios for the distribution along the x axis (left) and the y axis (right) as a function of the distance from the detector to the projection plane, after subtraction. The distribution along y axis is fitted with a 2nd order polynomial in the interval around minimum.

Results

2nd run

Determination of the cube's width.

real width=50 mm.

At D^x=266.06 mm and D^y=242.86 mm:

$FWHM^x$=81.6 ± 3.67 mm.
$FWHM^y$=86.98 ± 3.49 mm.

$2\sigma^x$=69.3 ± 3.25 mm.
$2\sigma^y$=73.87 ± 3.18 mm.

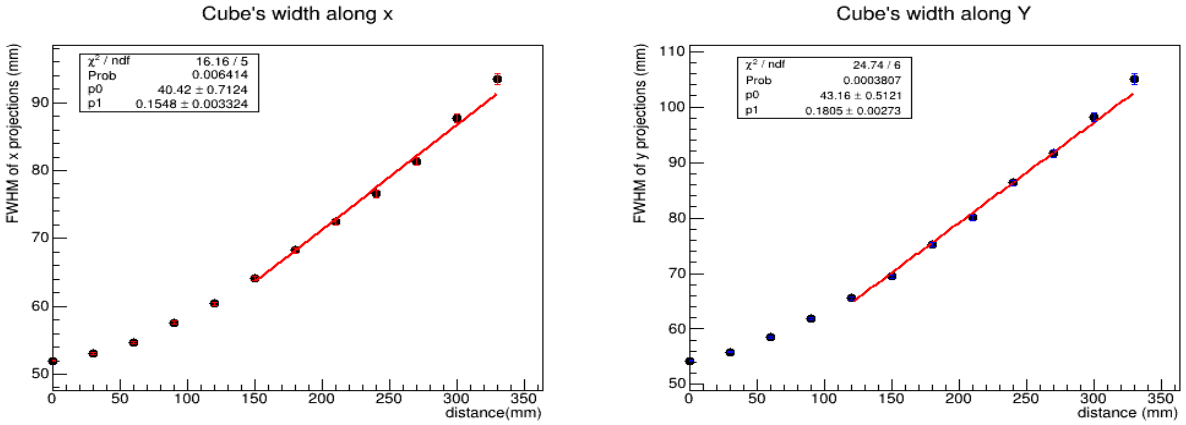

(a) The FWHM (mm) of x and y projections.

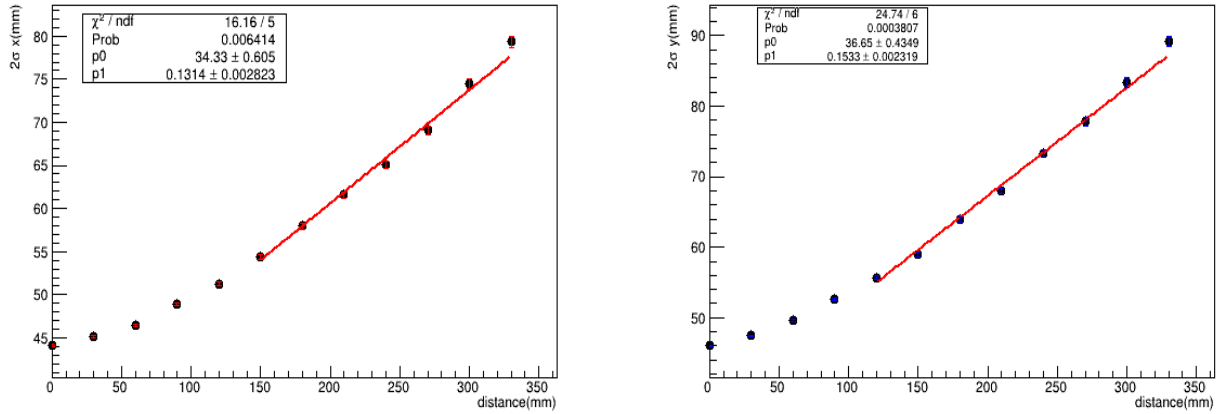

(b) 2σ (mm) of x and y projections.

Figure 23: (a)The FWHM(mm) and (b) The 2σ (mm) of the projections along x (left) and along y (right) as a function of distance (mm) in 2nd run.

Presentation Outline

- Introduction
- The experimental set-up in the laboratory
- Data Analysis
  - Track Reconstruction
  - Back Projection Method
  - Results
- Conclusions and future work

Conclusions and future work

To conclude...

- The Muon Radiography technique can be applied for the imaging of geometrical objects of smaller scale.
- The Back-Projection method finds the approximate distance of the object from the detector.
- The cube's dimensions seem to be overestimated by this method.

What can be next..

- The method can be tested for different geometrical objects and distances.
- Optimization of the tracking method.
- The Muon Scattering Tomography (MS) can be also applied for the imaging of the cube.
- New MICROMEGAS detectors 0.5 m x 0.5 m are under construction and will be set up in the next months in the framework of EKATY project for the application of muon tomography to archaeological sites.

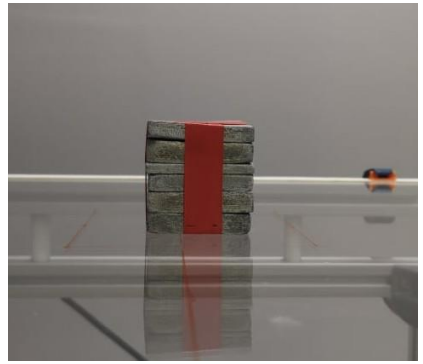

Figure 24: The lead cube.

Acknowledgements

I would like to express my special thanks to the members of Muon Tomography team, especially to professor Sampsonidis Dimos, professor Petridou Chariclia and Dr. Christos Lampoudis for giving me the opportunity to get to know the field of muon tomography.

Also, I am grateful to the Doctoral student Ilia Kalaitzidou for providing me with her inspiring previous work on muon tomography.

Ilia Kalaitzidou. A feasibility study of muon tomography application in a non-invasive representation of tumulus, 2021.

Thank you for your attention!!

References

[1]Luis W. Alvarez, Jared A. Anderson, F. El Bedwei, James Burkhard, Ahmed Fakhry, Adib Girgis, Amr Goneid, Fikhry Hassan, Dennis Iverson, Gerald Lynch, and et al. Search for hidden chambers in the pyramids. Science, 167(3919):832–839, 1970.

[2]Lorenzo Bonechi, Raffaello D'Alessandro, and Andrea Giammanco. Atmospheric muons as an imaging tool. Reviews in Physics, 5:100038, 2020.

[3] Bonechi, L., D'Alessandro, R., Mori, N., & Viliani, L. (2015). A projective reconstruction method of underground or hidden structures using atmospheric muon absorption data. *Journal of Instrumentation, 10*(02). doi:10.1088/1748-0221/10/02/p02003.

[4] Bortfeldt, Jonathan. (2015). The Floating Strip Micromegas Detector. 10.1007/978-3-319-18893-5.

[5] GEANT4 collaboration, https://geant4.web.cern.ch/.

[6] Garfield++ toolkit, https://garfieldpp.web.cern.ch/garfieldpp/.

Back up slides
Energy deposition in 20cm Pb (GEANT4 Simulation)

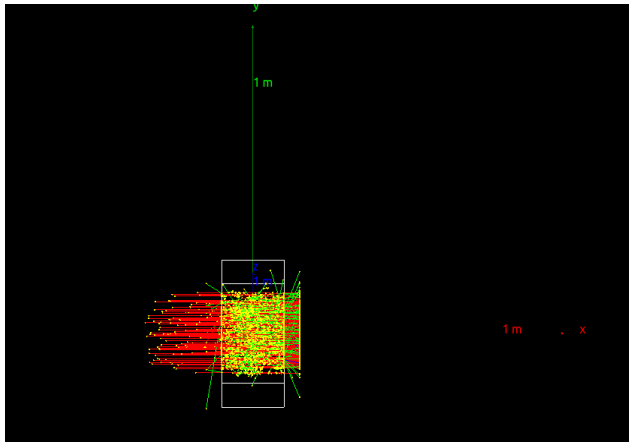

Figure 27: Muons pass through 20 cm Pb (GEANT4 simulation).

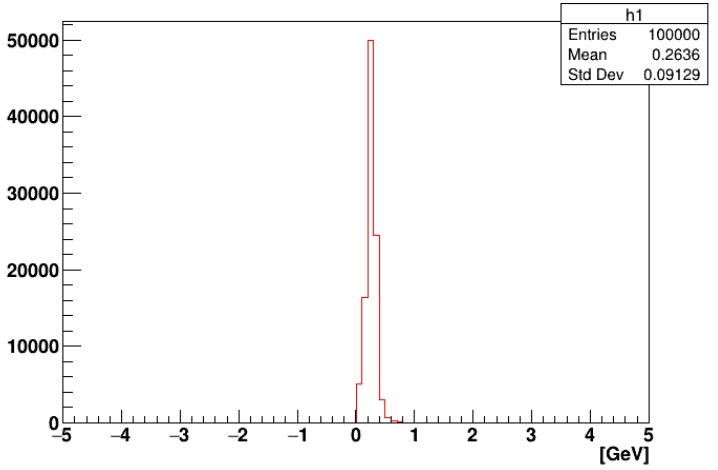

Figure 28: Energy deposition per muon in 20 cm Pb.

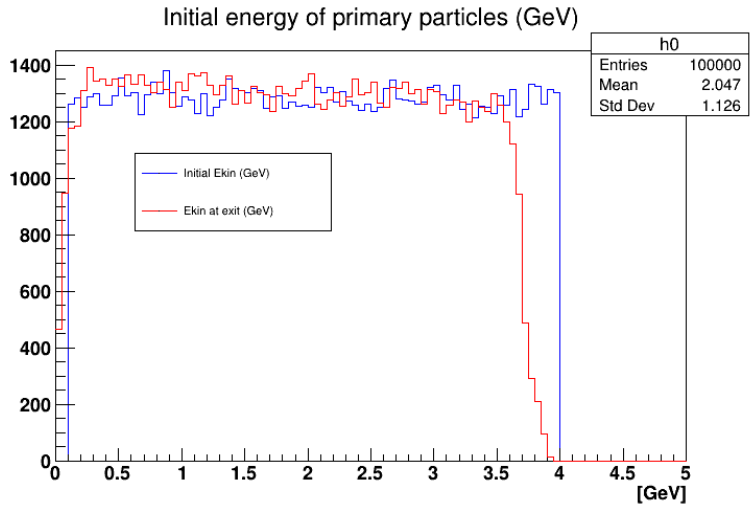

Figure 29: Initial and final energy (GeV) of muons traversing 20 cm Pb.

Back-up slides

Angular distibution of reconstructed tracks in 2nd run.

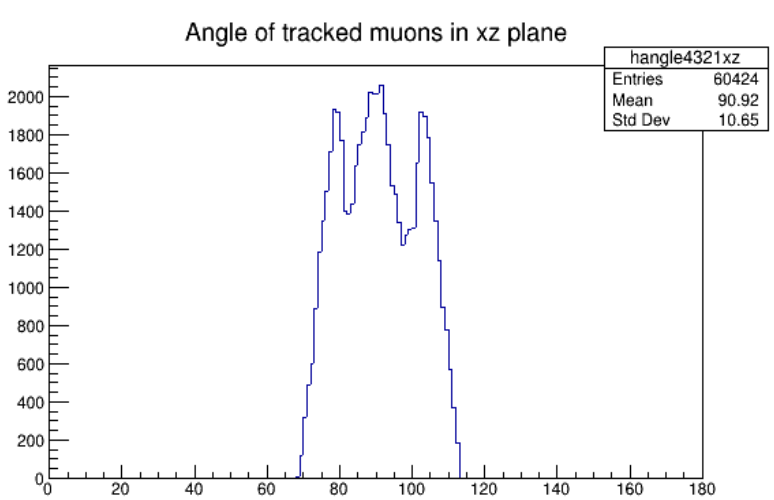

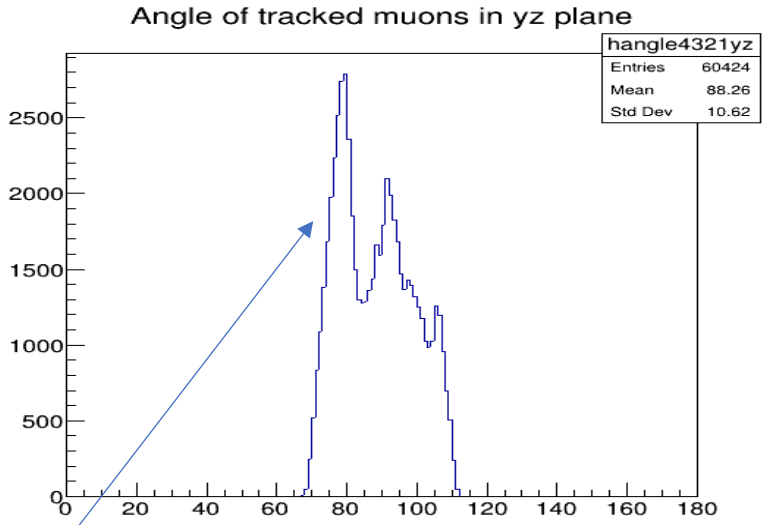

Figure 26: Angular distribution (deg) of reconstructed tracks with cube (data-2nd run).

Because of the asymmetry in yz plane-> Tracks with angle in the interval (82^o-100^o) have been taken into consideration.

Back-up slides

Calculation of errors.

- Errors in width-to-pitch ratio-> Standard deviation error.

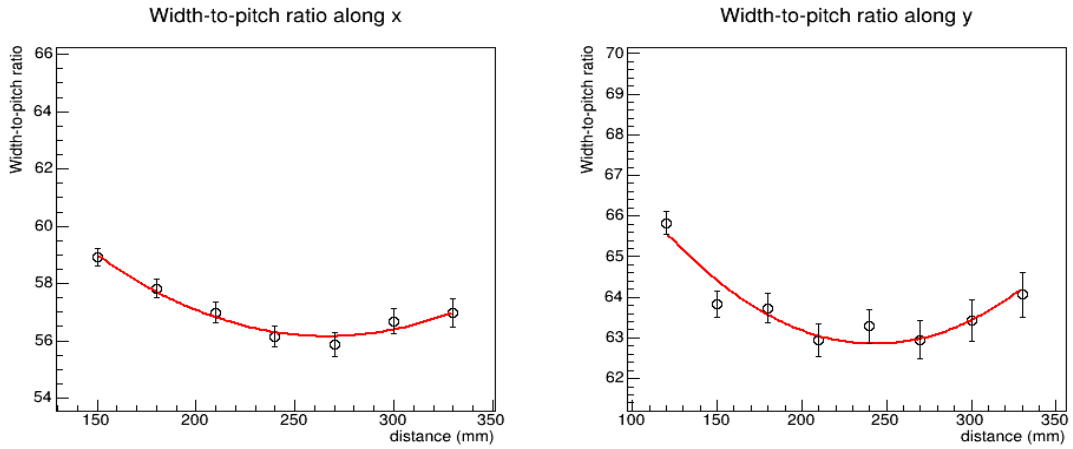

Figure 27: Width-to-pitch ratio with errors zoomed in the fitted region.

- Errors in FWHM->From error propagation: 2.355*(width-to-pitch ratio error)*pitch.

- Errors in the calculated distance along x and y axis-> Error propagation from covariance matrix of the fitted function.